Journal of Hydrology: Regional Studies 30 (2020) 100692

Contents lists available at ScienceDirect

Journal of Hydrology: Regional Studies

journal homepage: www.elsevier.com/locate/ejrh

Temporal and spatial variability of shallow soil moisture across four planar hillslopes on a tropical ocean island, San Cristóbal, Galápagos

Madelyn S. Percy[a,*], Diego A. Riveros-Iregui[b], Benjamin B. Mirus[c], Larry K. Benninger[a,d]

[a] Department of Geological Sciences, University of North Carolina at Chapel Hill, United States
[b] Department of Geography, University of North Carolina at Chapel Hill, United States
[c] U.S. Geological Survey, Geologic Hazards Science Center, Golden, CO, United States
[d] Department of Marine Sciences, University of North Carolina at Chapel Hill, United States

ARTICLE INFO

Keywords:
Temporal soil water record
Spatial soil water distributions
Hillslope soil water connectivity
Runoff generation
Galápagos climosequence

ABSTRACT

Study region: This paper provides a summary of findings from temporal and spatial studies of soil water content on planar hillslopes across the equatorial island of San Cristóbal, Galápagos (Ecuador).

Study focus: Soil water content (SWC) was measured to generate temporal and spatial records to determine seasonal variation and to investigate how the behavior of surface and near-surface root-zone soil water may support island-wide hydrogeology models. SWC probes were installed at four weather stations in a climosequence to generate a temporal record, and spatial surveys of shallow SWC across the selected sites were completed during wet and dry seasons. Temporal differences in SWC were driven by seasonal variations in rainfall and evapotranspiration, while spatial variability remained high during both wet and dry seasons. Unsaturated hydraulic conductivity determined by mini-disk infiltrometers was highly variable across the slopes, as were other hydrologic variables.

New hydrological insights for the region: The high heterogeneity of soil water and hydrologic characteristics provides a means to explain why little runoff is observed at the study sites: soils do not saturate uniformly across hillslopes, allowing for runoff generated in one part of the hillslope to be conducted into the soil in adjacent parts of the hillslope. The lack of connected surface runoff helps explain how water enters the groundwater system of the island.

1. Introduction

Knowledge of near-surface soil water content and the amount of water in pore spaces in the top of a soil (0 − 15 centimeters) contributes to the understanding of climate, energy balance, and plant health. Soil water content distributions across hillslopes can affect energy fluxes by: (1) controlling the partitioning of rainfall into evapotranspiration, runoff, and recharge (Mirus and Loague, 2013; Rasmussen et al., 2011); (2) facilitating soil development and changes in chemistry by serving as a means of solute transport and changing the oxidation state of soils (Bailey et al., 2014); and (3) serving as the source of water for soil microbiota (Graham et al., 2010). Soil water content distributions also affect hydrologic processes at varying scales (Western and Blöschl, 1999), ranging from

* Corresponding author at: 208 Mitchell Hall, CB 3315 104 South Road, Chapel Hill, NC 27599-3315, United States.
E-mail address: madelynp@live.unc.edu (M.S. Percy).

https://doi.org/10.1016/j.ejrh.2020.100692
Received 27 November 2019; Received in revised form 6 April 2020; Accepted 24 April 2020
Available online 30 May 2020

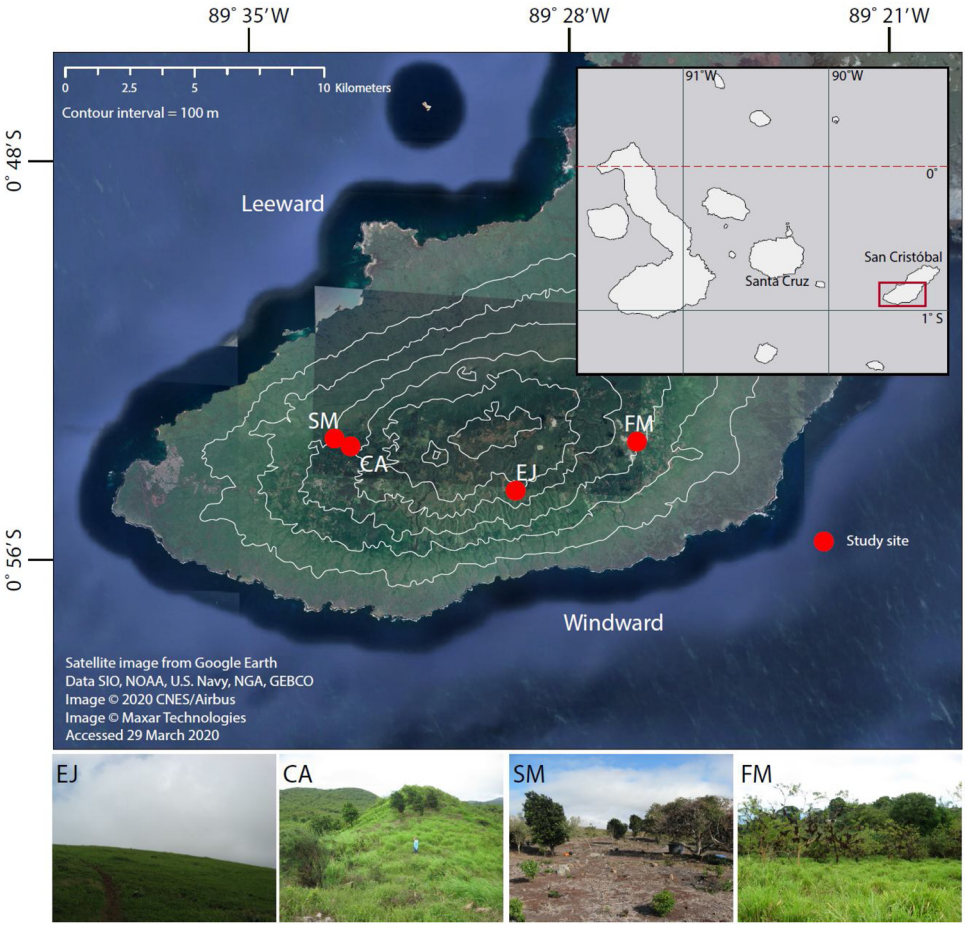

Fig. 1. Field sites, San Cristóbal Island (Galápagos). Satellite photo from Google Earth, isocontours adapted from Adelinet et al. (2018); contour interval is 100 meters. Field photographs for EJ (El Junco, taken 5 June 2015), CA (Cerro Alto, taken 20 May 2015), SM (Sitio Mirador, taken 17 October 2016), and FM (Finca Merceditas, taken 9 June 2015). 2015 photos taken during the wet season; the photo of SM was taken during the dry season.

centimeters (e.g., capillary flow versus macropore flow, solute transport) to kilometers (e.g., surface-atmosphere interactions, large-scale flooding). The distribution of soil water across hillslopes is affected by a number of factors, including season (Martinez et al., 2008; Western and Grayson, 2000), topography (Beven and Kirkby, 1979), flora (Chandler et al., 2018; Metzger et al., 2017), land use (Foster et al., 2003), and physical properties of the soil (Dong and Ochsner, 2018; Zhu and Mohanty, 2003). We investigated the effect of seasonal variations in rainfall and evapotranspiration on the temporal and spatial distributions of soil water on San Cristóbal, a tropical ocean island located in the Galápagos archipelago in the equatorial Pacific (Fig. 1).

Previous work on soil moisture patterns and dynamics has largely focused on subtropical or temperate landscapes, where a hillslope's aspect affects the soil water content, not just through evapotranspiration, but by fundamental changes to the hillslope's hydrology. Slope aspect affects the types of plants growing on the hillslope, the amount of solar radiation that each side of the slope receives during the summer and the winter, and the shape of the slopes (Pelletier et al., 2018). Authors have noted that polar-facing slopes (south-facing in the southern hemisphere and north-facing in the northern hemisphere) are usually cooler, wetter and steeper, while equator-facing slopes are drier and more likely to approach wilting point, and less steep (Ebel, 2013). Low-elevation equatorial sites, like those on San Cristóbal, are largely unaffected by aspect because solar radiation is direction-independent, providing an opportunity to explore the seasonal change, at constant aspect, in the distribution of soil water.

The relationship between temporal and spatial variability in soil water content based on season has been extensively studied in subtropical and temperate climates. The Shale Hills Critical Zone Observatory (Pennsylvania, USA) has served as the site of numerous spatial and temporal soil water surveys. The results of the temporal studies show that while root-zone and shallow soil water probes (less than 0.3 m deep) recorded strong seasonal differences in the distributions of soil moisture, deeper soil moisture probes (inserted to depths between 0.3 and 1.1 m) showed greater temporal persistence (Takagi and Lin, 2012). At the Wüstebach catchment in Germany, authors noted that seasonal, and even event-driven variations in precipitation affected the topsoil's soil moisture content, while deeper soil water content was affected by the depth to the water table more than the local precipitation (Rosenbaum et al., 2012). A study of soils in France, Spain, and Tunisia found that while precipitation caused the mean soil water content across a field

to change, the distribution of soil water, especially minima and maxima, remained constant through time (Vachaud et al., 1985). Other authors have noted similar examples of spatially heterogeneous soil water distributions that are stable inter- or intra-annually (Brocca et al., 2009, and references therein; Grayson et al., 1997). At all these sites, an extensive network of soil moisture monitoring probes, weather stations, and groundwater observation wells and piezometers were in place, facilitating detailed quantitative understanding of the temporal and spatial dynamics of soil moisture.

Tropical sites like the Galápagos often lack the scientific infrastructure to support studies like those carried out in subtropical and temperate climates, despite the importance of the temporal behavior and spatial distribution of soil water to the island-wide hydrology. Previous studies have used electromagnetic resistivity (D'Ozouville et al., 2008a), seismic refraction (Adelinet et al., 2018), numerical modeling (Domínguez et al., 2016, 2017), and noble gas and stable isotope geochemistry (Warrier et al., 2012) to create a conceptual model for the behavior of water as it enters the groundwater system (summarized in Percy et al., 2016). In general, the current conceptual models of the island's hydrogeological system require that water infiltrates through soils and into perched aquifers that either drain via springs to the surface or deeper into the island's groundwater system. However, little work has been done to understand the behavior of shallow soil water across the island's planar hillslopes. San Cristóbal's seasonal variability in precipitation amounts and type (Percy et al., 2016; Schmitt et al., 2018) makes it a prime study site to understand how seasonal variability affects the temporal and spatial behavior and distribution of soil water across hillslopes on a tropical island.

This study uses new data collected from soil moisture and weather monitoring stations at four different altitudes on San Cristóbal, coupled with intensive spatial sampling of shallow soil water content distributions across these four hillslopes during two different seasons, to address three primary questions:

1 Does the soil water saturation differ seasonally on the studied hillslopes?
2 Do we observe differences in the spatial patterns of near-surface soil water content across these hillslopes based on seasonal differences in stochastic variables like rainfall and evapotranspiration?
3 Could spatial patterns of shallow soil water affect runoff generation?

Through geostatistical analysis of spatial patterns, time-series analysis of the hydrologic response monitoring across the hillslopes, and characterization of soil hydraulic properties, we provide further insights into variations in the hillslope-scale water balance across a climosequence in a tropical equatorial island setting.

2. Methods and materials

2.1. Site selection and description

San Cristóbal Island, a basaltic volcanic island that is part of the Galápagos Archipelago (Fig. 1), is estimated to have emerged from the Pacific around 2.4 Ma (Geist et al., 2014), and the youngest dated eruption on the southwest side of the island, where our study sites are located, occurred 0.65 Ma ago. The bedrock across the archipelago is basaltic and ranges from tholeiitic to alkaline in nature; across San Cristóbal, at least six mineralogically and chemically distinct basalts were identified that range in age between 2.35 ± 0.03 and 0.7 Ma on the southwest side of the island to nearly modern on the northeast side of the island (Geist et al., 1986). Despite its equatorial latitude, San Cristóbal experiences seasons due to the latitudinal migration of the Intertropical Convergence Zone (Trueman and D'Ozouville, 2010). From January through May, San Cristóbal generally experiences weather typical of the tropics, with large convective rainstorms across the entire island. From June until December, southeast trade winds blow across cool upwelled ocean water to create an inversion layer, resulting in a dry and sunny coastal zone while the summit at roughly 700 m above sea level receives rainfall and is often cloudy (see Schmitt et al., 2018, for details of upland climate). The seasonal shift from highly variable, island-wide precipitation to consistent, highland-only precipitation has resulted in a climosequence that is strongly dependent on elevation, ranging from very arid at the coastline to very humid at the summit (Colinvaux, 1972). Vegetation ranges from native scrub and cacti at the coastline to grassy pastures, broadleaf shrubs, and trees at middle elevations, and native herbs and shrubs at the highest elevations (Huttel, 1986).

We selected four hillslope sites across the island, co-located with weather stations deployed in 2015 (Fig. 1), two on the windward side and two on the leeward side. The weather stations were installed to capture as many climate zones as possible while facilitating routine maintenance, instrument security, and data downloads. El Junco (EJ) is the highest site on the windward side of the island and is located in the very humid zone. The hillslope is convex-linear (see classification of Schoeneberger et al., 2012, for explanation of slope shapes) and is bounded on the east side by a bedrock outcrop. The studied portion of the slope covers an area of 48 × 50 m^2. Sitio Mirador (SM) and Cerro Alto (CA) are located on the leeward side of the island and span the transition zone between dry (SM) and humid (CA) climates. CA's slope shape is convex-concave and has cow paths that we observed to affect runoff at the site; the studied portion of the slope is 54 × 40 m^2. SM, with a study area of 96 × 40 m^2, is the most gently sloping of the sites and is bounded on three sides by bedrock cliffs. Finca Merceditas (FM) is the lowest site, but because it is on the windward side of the island, it remains in the transition zone between the dry and humid climate zones. The slope shape at FM is linear-linear and was partially covered by a study area of 75 × 50 m^2. With these four sites, we have hillslopes in most of San Cristóbal's climate zones except for the arid zone. The arid coastal zone's soils are thin and unevenly distributed, found mostly in cracks in lava flows, and so are not included in this study.

We visited the sites during the Galápagos wet season of 2015 and the dry season of 2016; wet season 2015 was during an El Niño and was wet (161 mm of measured precipitation at EJ over five weeks of the study period, from the weather station at each site),

Table 1
Site description.

	Elevation (m)	Climate zone	Slope shape [a]	Average slope angle [b]	Slope length [c] (m)	Land use
El Junco (EJ)	620	Windward; wet	Convex-linear	16.0 ± 8	48	National park land, close to foot path
Cerro Alto (CA)	520	Leeward; transition	Convex-concave	26.4 ± 15	54	Cow pasture
Sitio Mirador (SM)	414	Leeward; dry	Linear-linear	14.0 ± 9	96	Cow pasture to garden, bare soil
Finca Merceditas (FM)	320	Windward; transition	Linear-linear	17.0 ± 9	74	Cow pasture; citrus and guayaba orchard

[a] Schoeneberger et al. (2012).
[b] Average slope angle calculated from the mean of the measured slopes between points from kriged elevation map in ArcGIS.
[c] Slope length is the length of the longest downslope transect at each site.

while the study during 2016 occurred during an eight-month drought (46 mm of precipitation measured over the eight-week study period at EJ). Summary details about each site are provided in Table 1. Between the field seasons, a wildfire affected CA and SM, probably in July according to farmers. At CA, the majority of the sampling points were unaffected by the wildfire and the site remained a pasture; only the downslope points experienced the fire. SM's land use changed following the fire from a carefully maintained natural area that served as a nursery for native plants to a garden with little ground cover.

2.2. Measurement of climate variables and temporal soil water data

The deployed weather stations collected data on rainfall, wind speed and direction, relative humidity, temperature, and solar radiation, and were co-located with soil moisture probes at three depths. Data gaps at the stations were the result of inclement weather and biological activity that resulted in the failure of instruments. To record the volumetric soil water content, we installed soil water sensors (Model CS616, Campbell Scientific Inc., Utah, United States) horizontally at depths of 10, 20, and 40 cm at EJ, and 10, 20, and 30 cm at the other three sites. However, because of equipment failure after deployment, continuous soil moisture data at SM are not available. The data were recorded every 15 min, with the exception of the station at FM which recorded data every 5 min for the first 300 days. A complete description of the equipment used to measure climate variables is found in Schmitt et al. (2018).

To calculate the reference evapotranspiration rates, we used the FAO Penman-Monteith method (Zotarelli et al., 2010) because of the available weather station data. We used the grass reference surface in our calculations because none of the weather stations were installed under trees and because three of the four sites were grassy, while the last site (EJ) is characterized by low herbs.

2.3. Physical properties and site characterization

We made hillslope-scale and point measurements to describe the physical properties of the studied hillslopes. We recorded physical variables at each point for which near-surface soil water content was collected, as described below. Digital elevation models available for San Cristóbal were insufficient because their resolution was too coarse for this study (20 m from ENVISAT, D'Ozouville et al., 2008b), so we surveyed the four hillslopes across the 2-m grid via tape-and-compass measurements (Fig. S1). From the generated 2-m resolution DEM, we calculated the slopes and upslope accumulation area for each site using ArcGIS (Esri, 2011). We noted the overlying plant type (bramble, fern, herb, grass, tree, and bare soil) at the point at which we inserted the soil water content probe, and recorded the presence of trees, tree roots, or rocky outcrops within 2 m of each measurement point. We present maps of the plants at each measurement point for both seasons in Figure S2. We used a soil step probe (33″ Plated Step Probe with Handle, AMS, Idaho, United States) to measure the depth of soil (hereafter, depth to refusal) after measuring the soil water content at each point. Excavations show that the depth to refusal is the depth to a clay-rich horizon or rock and provide an adequate proxy for the depth to which soils are heavily rooted. Maps of the depth to refusal are presented in Fig. S3.

2.4. Soil water content and hydrologic properties

During the field seasons, we measured the near-surface soil water content using a Hydrosense II (HS2) CS659 portable soil water content probe (12-cm rods, Campbell Scientific Inc., Utah, United States) with a support volume (the volume of soil over which the soil water content is measured) of approximately 460 cm^3. The output from the HS2 is electrical period (microseconds, μs) and a conversion is used to calculate volumetric water content (volume%). The period is strongly related to the dielectric permittivity of the material around the probe rods (Campbell Scientific Hydrosense II User Guide). Tropical soils on volcanic parent material can have a range of clay and amorphous material contents that will affect the calibration of soil water content probes (Noborio, 2001; Regalado et al., 2003), so we noted both period and calculated soil water content. We calibrated the HS2 in the laboratory using minimally disturbed soil core samples collected in 130 cm^3 metal cylinders.

In the 2015 wet season, we took at least 100 shallow soil moisture measurements within a 20 × 20 m^2 grid to provide adequate spatial coverage on the small hillslopes. We made additional measurements down slopes in transects extending from grid lines. The dry season campaign in 2016 included the same 100 points measured during the 2015 campaign. We measured additional points during both field campaigns that are included in the geospatial analysis. We collected measurements over several days at each site; during the wet season campaign, the weather stations were not yet operational at EJ, CA, and FM, but field notes indicate that it rained every day at EJ and for one of the six measurement days at CA. During the dry season, only EJ received rain during data collection (Fig S4).

We also measured hydraulic properties of the soils to support the temporal and spatial observations of the soil's volumetric water content. To measure the hydraulic properties of the soils on the four hillslopes, we used in situ experiments to quantify the unsaturated hydraulic conductivity and laboratory analyses to measure bulk density, grain size distributions, pH, and the weight percentage of amorphous material in the soils. In the field, we measured the sorptivity of water and unsaturated hydraulic conductivity using Meter Group mini-disk infiltrometers (MDI) with an applied suction of −2 cm for sites CA, SM, and FM, and −0.5 cm for site EJ (due to slow infiltration across the site). We applied the MDI to the soil after clearing the leaf litter and made at least two measurements of unsaturated hydraulic conductivity within 1 m of each other at SM and FM. We used the Excel macro provided by the manufacturer to calculate the sorptivity and unsaturated hydraulic conductivity. We measured the bulk density of the soils using the saran method (Blake and Hartge, 1986) to aid in the calibration of the Hydrosense II, as well as estimate what the maximum volumetric water content could be. We calculated the bulk porosity in samples from the sites using an average particle density value of 2.60 g/cm^3, the average density of kaolinite, gibbsite, halloysite, and illite, all of which are expected to be important components

of the soil (porosity = 1 – [bulk density/particle density]). In the laboratory, we measured grain size distributions from each site by dry sieving the fine earth fraction (< 2 mm particles) on a shaker, followed by gravimetric determination to yield the percent of the total weight of the sample, with chemical dispersion of clays accomplished using sodium hexametaphosphate (Soil Survey Staff, 2014). The pH of the mineral soil was measured by combining 5 g of fine earth mixed in 20 mL of distilled water and allowed to equilibrate for at least one hour before allowing the particles to settle and measuring the pH of the supernatant (Pansu and Gautheyrou, 2006). Naturally occurring amorphous materials in soils are noncrystalline and poorly crystalline material, usually composed of compounds of Si, Fe, and Al that coordinate with free oxides and hydroxides. We measured the weight percentage of amorphous material in the bulk soil using the ammonium oxalate extraction method (Jackson et al., 1986) at least once per site because amorphous materials can adsorb water and affect the hydrophobicity of soil.

2.5. Data processing

We analyzed the soil water content and climate time-series data using R computing software (R Core Team, 2017). To examine relative temporal changes in soil moisture, we normalized the measured volumetric water content to the maximum observed values during saturation to calculate relative soil saturations. To examine the observations spatially, we used semivariogram analysis to calculate the autocorrelation distance across the four sites during each season; semivariograms show the autocorrelation over distance across hillslopes and can be used to understand the distributions of soil water (Western et al., 2004). Understanding autocorrelation distance at the four sites provides a quantitative metric for the degree of hillslope connectivity, which is important to the understanding of runoff generation on the hillslopes. We input our gridded data into the geoR package in R (Ribeiro and Diggle, 2001) to test omnidirectional, exponential (Western et al., 2004) and spherical models (Bi et al., 2009). Different studies have found that the exponential or spherical models fit data better in different landscape types: the exponential model's covariance along the sill asymptotically approaches zero variance, while the spherical model's sill represents where the covariance is zero. We compared the raw output data from the HS2 (period) and the calculated soil water content to complete the semivariogram analysis using the different models. We tested correlation relationships between soil water content and topographic measures, including slope and upslope accumulation area, and the depth to refusal. We also analyzed the relationship between hillslope-averaged variables like bulk density, pH, fraction of amorphous material, unsaturated infiltration rates, soil texture, and the mean soil moisture and standard deviation of the soil water content for the wet and dry seasons.

3. Results

3.1. Temporal record of soil moisture

The temporal record of rainfall, soil moisture, and evapotranspiration is presented in Fig. 2 for sites EJ, CA, and FM. Summary data from the weather stations at all four sites are in Table 2. The wet season on San Cristóbal usually falls between January and May, and the dry season falls between June and December, with interannual variability in the beginning and end of the seasons. However, the beginning of the study fell within the strong 2015−2016 El Niño, which ended in May–June 2016 (Hu and Fedorov, 2019), resulting in very wet conditions throughout the first part of the study. As shown in Fig. 2a, almost 65% of the precipitation at EJ fell between October 2015 and February 2016. During this period, the wind was at its most variable, and the solar radiation was lower than during dryer parts of the year. On the island of Santa Cruz, researchers found that fog can account for approximately 20% of the net precipitation at high elevation sites at comparable elevations to EJ (Pryet et al., 2012b). Because of the configuration of the weather station, we did not measure the amount of occult precipitation at EJ, which means that an important source of water into the hillslope is not considered within the precipitation data. Within the soil, the deepest soil moisture probe (40 cm) recorded soil moisture levels that regularly approached saturation; the data show that soil moisture decreased more slowly from saturation than the shallow soil moisture. The dry period (February 2016 until the end of the data record, January 2017) had fewer rainstorms and the reference evapotranspiration was higher due to both higher windspeeds and greater solar radiation. This corresponds with a decline in the recorded soil moisture through the season, with rainstorms resulting in sudden increases in the shallower soil moisture data (10 and 20 cm) and much smaller increases in the deep soil moisture data (40 cm).

CA (Fig. 2b), located on the drier leeward side of the island, receives precipitation from large convective storms, rather than the fog that characterizes the "dry" season at EJ. In calculating the reference ET for site CA, the solar radiation term of ET was consistent across the year, but the wind term was highly variable and was the dominant control of the calculated reference evapotranspiration for the site. The data recorded by the soil moisture probes at CA show that the deepest soil moisture probe (30 cm) most often approached saturation, and the 20 cm deep probe was only slightly drier. The shallow probe (10 cm) recorded the greatest percent change in measured soil water content after precipitation events compared to the deeper soil probes and also indicated that the soil dried most quickly near the surface.

At the low-elevation windward site FM, the average reference ET remained around 2.40 mm/day throughout the seasons, in part because the windspeed remained consistent throughout the seasons. Changes in the daily reference ET are due to changes in radiation fluxes. The soil moisture data show that the shallowest soil moisture probe (10 cm) recorded the highest saturation across the study period, while the two deeper soil moisture probes (20 and 30 cm) had similar saturation values recorded through time.

At all of the sites, the temporal soil moisture record reflects different responses to precipitation events. For example, at EJ (Fig. 3a), the surface soil moisture probe at 10 cm showed a daily decline in the percent saturation until a large event, at which point the record reflects an increase to 100% saturation. The 10- and 20-cm probes first responded to the storm event at the same time;

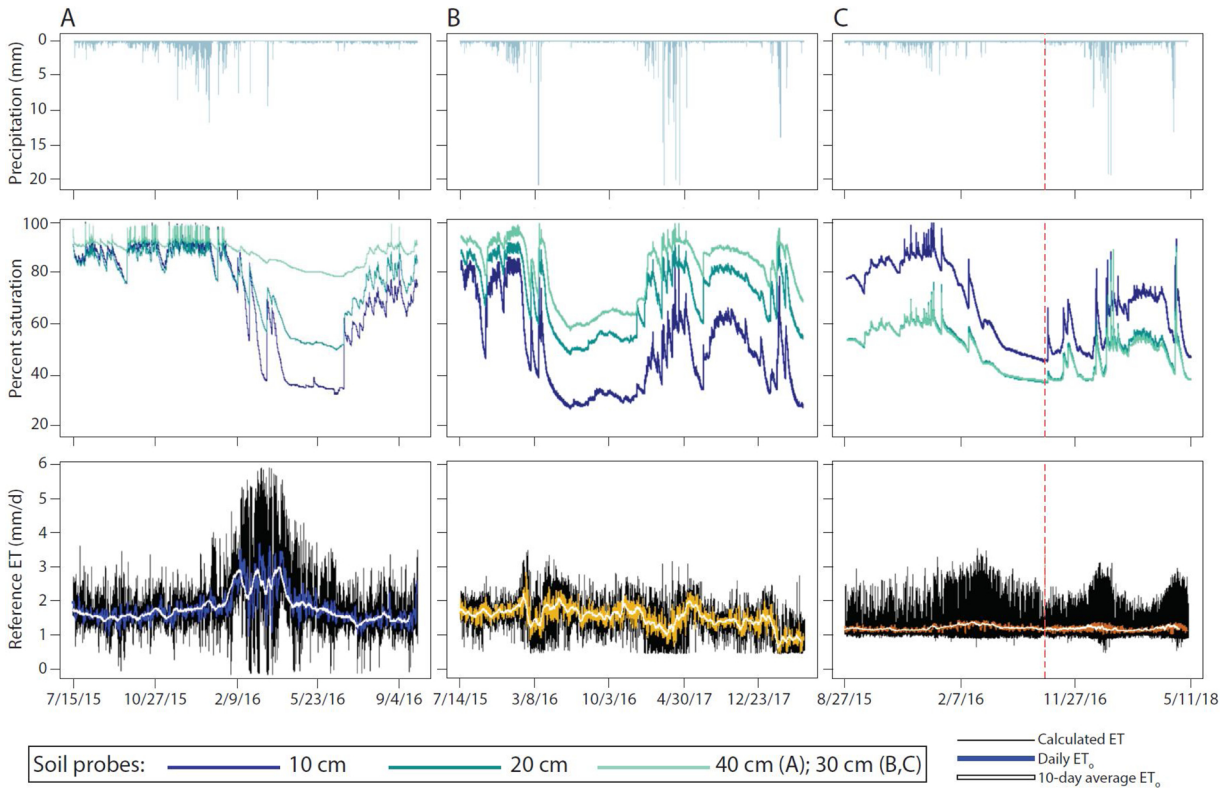

Fig. 2. Time series data including precipitation data, in millimeters, percent saturation at different depths, and calculated reference ET for (A) EJ, (B) CA, and (C) FM. Percent saturation was calculated relative to the highest recorded soil water measurement: (A) EJ – 60.7%, (B) CA – 77.2%, (C) FM – 57.5%. Different colors in the percent saturation plots represent the different depths of the soil moisture probes. The dashed vertical line in (C) represents the change in recording interval from 5 to 15 min.

however, the 20-cm deep probe did not record as steep of a rate in the increase of saturation. The 40-cm probe had the highest percent saturation prior to the storm event and did not respond to the storm event until hours after the surface soil probes. Several days after the precipitation event, the 40-cm deep probe reached saturation during smaller precipitation events, while the 10- and 20-cm soils had lower percent saturation values. Fig. 3b shows the response in percent saturation at CA to two storm events. The first storm event resulted in a nearly simultaneous increase in the percent saturation at all three probe depths within 30 min after the start of the event, indicative of preferential flow in the surface soil which may be an important mechanism at this site. The second storm event was recorded by all three soil probes simultaneously (within the same 15-minute measurement period). At CA, the surface soil dried most quickly. At FM (Fig. 3c), the 10-cm deep probe recorded the highest percent saturation throughout the considered time period, while the 20- and 30-cm deep probes recorded very similar percent saturations. The shallowest probe recorded an increase in the percent saturation approximately 50 min before the 20- and 30-cm root-zone probes began to record an increase in the percent saturation. The second, smaller event did not affect the 30-cm deep probe, and only marginally increased the percent saturation for the 20-cm deep probe but resulted in a 3% increase in the percent saturation for the surface probe, from 92% saturation to 94.8% saturation.

3.2. Spatial soil water patterns and statistics

The number of sampling points and summary statistics of the spatial soil water survey measurements (Table 3) show that the mean, maximum, and minimum measured values of soil water content during the wet seasons are, not surprisingly, higher than during the dry season. The standard deviation and coefficient of variation (a measure of the relative variability of the soil water content) are higher for the dry period than they are for the wet period at all four sites. While changes in soil water between field seasons are associated with the precipitation, the cross-site relationship between site-wide precipitation and mean soil water content is not linear, likely because of differences in physical properties of soils at the sites. For example, despite its location in the very humid highlands and the highest annual precipitation record, EJ has the lowest mean of spatial soil water content for the wet season, and the second highest mean of spatial soil water content for the dry season. CA's mean of spatial soil water content is the second highest during the wet season but has a low mean of spatial soil water content during the dry season. SM and FM display similar means of spatial soil water values during the wet season, but because SM is on the leeward side of the island and FM is on the windward side, the mean of the spatial soil water content during the dry season is higher at FM than SM.

Table 2
Weather station data.

Site	Elevation (m)	Avg. daily precip. (mm)	Mean annual temp (°C)	Avg. daily solar rad (kW m^{-2})	Avg. windspeed (m/s)	ET_O (mm/d)	Avg. annual surface soil% saturation	Avg. annual 20-cm soil% saturation	Avg. annual deep soil% saturation [a]*
El Junco (EJ)	620	44.96	20.20	0.13	2.9	1.91	69.5	76.9	89.1
Cerro Alto (CA)	520	22.81	22.00	0.18	3.7	1.57	49.1	71.0	81.2
Sitio Mirador (SM) [b]§	414	2.49	22.38	–	–	–	–	–	–
Finca Merceditas (FM)	320	11.53	23.38	0.15	1.5	2.47	67.5	49.9	49.4

[a] *Deep soil moisture probes were installed at 30 cm depth at CA and FM and 40 cm depth at EJ. [b] §Sensors at SM failed early in the experiment and do not provide meaningful data beyond precipitation and temperature.

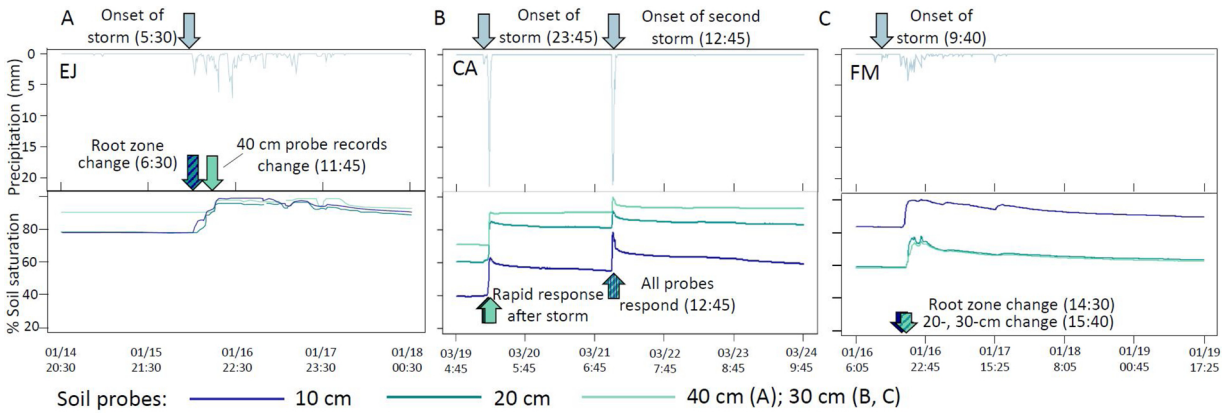

Fig. 3. Response of measured soil saturation to precipitation events at (A) EJ, (B) CA, and (C) FM. The time of precipitation onset and response by soil water probes are in the figure, except for (B), when the response to the first storm at all depths were recorded within 15 min of 00:15, while the response to the second storm was recorded at 12:45 on 21 March. Times on the x-axis are based on 15-minute recording intervals for EJ and CA and 5-minute recording intervals for FM.

Table 3
Summary of the soil moisture patterns observed at the four study sites.

Site	Season	Days*	Points†	Soil water content (volume%)				Standard deviation	Coefficient of variation (%)	Skewness coefficient	Kurtosis coefficient
				Maximum‡	Minimum	Mean	Median				
El Junco (EJ)	Wet	3	206	50.9	28.1	42.7	42.8	4.16	9.73	−0.717	0.488
	Dry	4	280	47.5	6.3	24.1	23.9	6.63	15.51	0.359	0.062
Cerro Alto (CA)	Wet	6	253	52.2	39.4	47.3	47.7	3.15	6.65	−0.516	−0.524
	Dry	4	211	36.9	6.7	17.6	17.0	4.45	25.24	0.964	2.465
Sitio Mirador (SM)	Wet	2	180	52.2	35.8	46.2	46.9	4.37	9.45	−0.417	−0.763
	Dry	4	328	36.6	0	15.7	15.9	5.88	37.40	0.235	0.739
Finca Merceditas (FM)	Wet	3	211	52.2	43.3	50.2	50.5	1.63	3.24	−1.485	3.124
	Dry	4	302	38.6	2.8	25.4	25.5	4.23	16.67	−0.559	2.426

*Number of days spent measuring the soil moisture across the sites. †Number of points measured during each field season at each site. ‡Maximum value reported by the Hydrosense II is 52.2% soil water content.

There are no easily discernible spatial patterns in the distribution of near-surface soil moisture across the hillslopes (Fig. 4). At EJ, the most humid site, neither of the spatial surveys show a relationship between soil moisture distribution and topography across the hillslope, although the lower portion of the slope for the dry season was slightly wetter than the upper portion of the slope, collected the day before, because of a rainstorm that occurred on the day we made the measurements on the low slope segment (Supplementary Fig. 4). Any possible pattern present at CA is difficult to identify because of the rock faces and thin soils that dominate the middle of the hillslope at this site. In the areas with spatially continuous data, soil moisture increased slightly in the middle of the saddle at the top of the hill at CA, at a point with the greatest convergence at the study site. For SM, the distribution of soil moisture appears random during both the wet and dry season, although less data were collected during the wet season. The noticeably wet area at SM during the wet season occurred where taller trees and thick herbs shaded the ground. At FM, the distribution of soil moisture appears random during both the wet and dry seasons.

The distribution of the soil water content data varies from site to site, with the Shapiro-Wilk test of normality indicating that none of the sites' soil water content distributions are normal. Previous authors used the gamma distribution (e.g., Kaiser and McGlynn, 2018) to describe the probability distribution of data because it resembles the positive skewness often observed with soil pore size distributions (Tuller and Or, 2005) and it has been experimentally tested in a variety of catchments (e.g., McGuire et al., 2005). We examined histograms of the soil water content for each site and applied gamma distributions (Fig. 5). For all but FM, the dry season's distributions are positively skewed, while for all of the sites, the wet season's distributions are negatively skewed. Other studies note that negative skewness is observed when the bounded function approaches the upper bound of porosity and the soil water content has reached saturation (Kaiser and McGlynn, 2018; Western et al., 2002), whereas positive skewness corresponds to the soil water content approaching the wilting point.

We tested the temporal stability of the soil moisture spatial distributions by ranking the soil moisture values and comparing the ranks of the points that we measured during both seasons. Across the four sites, there was no temporal stability in the spatial distribution of soil moisture. However, it is crucial to note that other studies that have observed temporal stability of soil moisture distribution patterns incorporated significantly more time points, including studies that collected soil moisture data over years (Dari et al., 2019; Gao et al., 2019; Starks et al., 2006; Western et al., 1999). Additional interpretations of the temporal stability of soil moisture distributions across our hillslopes would require additional spatial surveys of the slopes to capture not just wet and dry

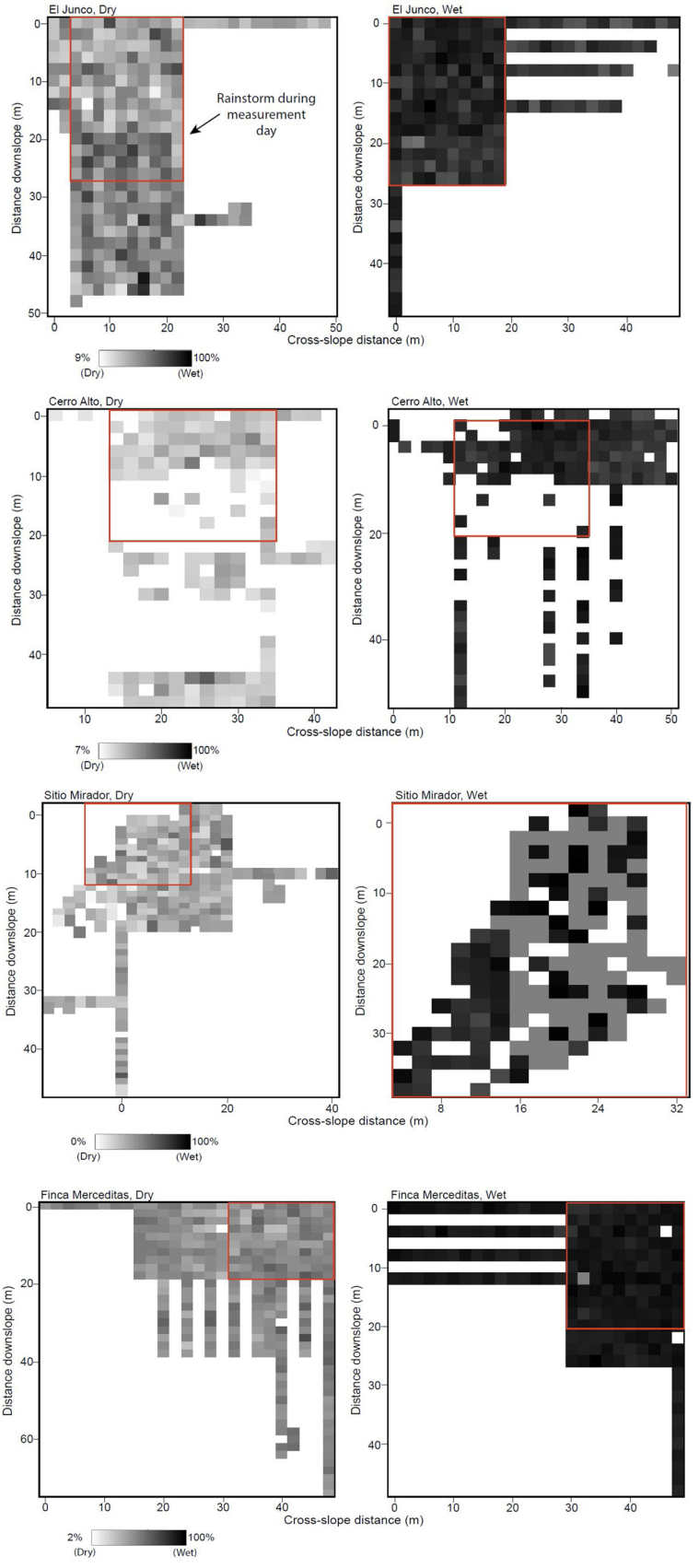

(caption on next page)

Fig. 4. Maps of soil saturation for the dry (left column) and wet (right column) seasons. Each pixel represents one soil water measurement that was then converted to percent saturation by dividing the measured value by the maximum measured soil water content from the weather station. Blank spaces represent areas where no soil water data are collected. Red boxes indicate areas that we measured in both dry and wet seasons. At EJ, the change in the percent saturation during the dry season is the result of a heavy rainfall; where the rain affected the data is indicated with an arrow. (For interpretation of the references to colour in this figure legend, the reader is referred to the web version of this article.)

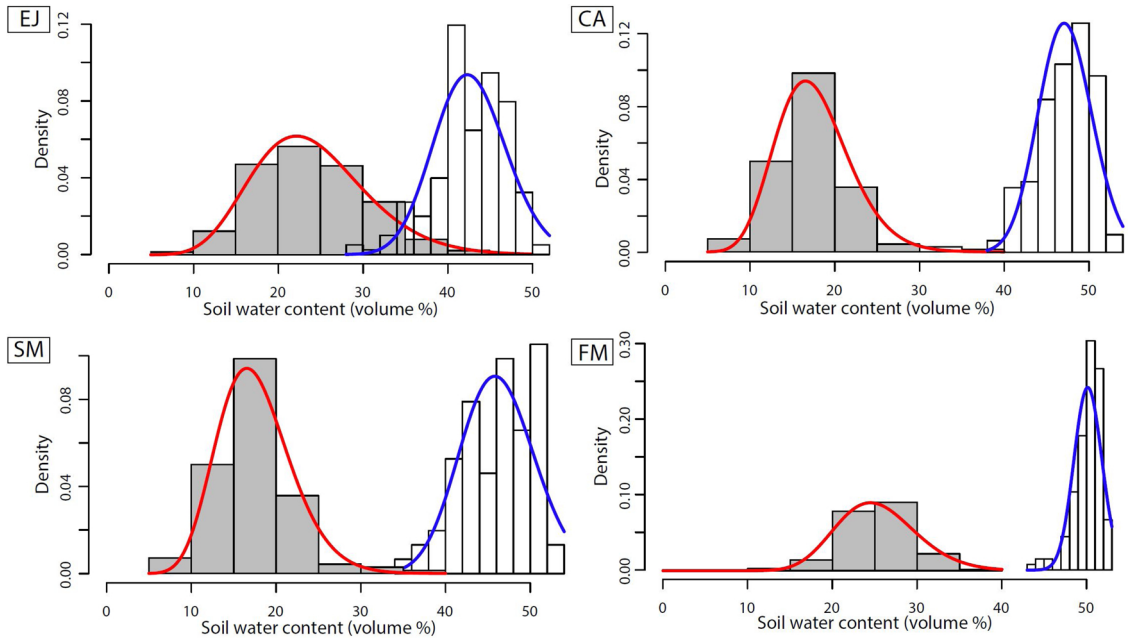

Fig. 5. Histograms and fitted gamma density functions of soil water content for each site. The white histograms and blue density functions correspond to the wet seasons and the gray histograms and red density functions correspond to the dry season. The distributions reflect the range of spatial measurements, although the maximum value reported by the probe is 52.2% soil water content because of the calibration equation used in the Hydrosense II. Differences in the binning interval between the wet and dry season reflect the greater number of data points for the dry season. (For interpretation of the references to colour in this figure legend, the reader is referred to the web version of this article.)

seasons, but the transition between the seasons.

3.3. Geostatistical analysis

We used semivariogram analysis at each site to evaluate spatial correlations between measured soil moisture. We made the models of semivariance using the directly measured period (μs) rather than the calculated soil water content because the Hydrosense II does not report volumetric water content values above 52.2% due to internal calibration within the sensor, while the measured period is reported from the sensor for every point. The soil's electrical response is affected by soil moisture, but also by the clay content, organic material content, and soil salinity (Topp et al., 1980). While the use of period rather than volumetric water content affected the autocorrelation distances calculated with the semivariogram analysis, this introduced less error into the interpretations of the results because of greater spatial coverage across the hillslopes. We tested a range of input values for the nugget, the partial sill, and the range parameter, selected based on the measured data for each model semivariogram and reported the model with the lowest sum-of-squares fit. The values used for each of the best-fit models are in Table 4. The spherical model type provided a lower sum-of-

Table 4
Summary of the variogram model inputs of the soil moisture patterns from the four study sites.

Site	Season	Sample size	Model type	Σ^2	φ	Nugget	Sum-of-squares fit
El Junco (EJ)	Wet	206	Spherical	0.005	29	0.004	1.12×10^{-3}
	Dry	280	Spherical	0.015	30	0.009	7.55×10^{-3}
Cerro Alto (CA)	Wet	251	Spherical	0.003	29	0.001	2.74×10^{-3}
	Dry	211	Sph/Exp	0.002	20	0.002	8.02×10^{-3}
Sitio Mirador (SM)	Wet	180	Spherical	0.020	15	0.004	6.85×10^{-3}
	Dry	328	Exponential	0.012	45	0.010	1.14×10^{-2}
Finca Merceditas (FM)	Wet	211	Sph/Exp	0.002	25	0.002	2.46×10^{-3}
	Dry	302	Sph/Exp	0.002	30	0.003	3.05×10^{-3}

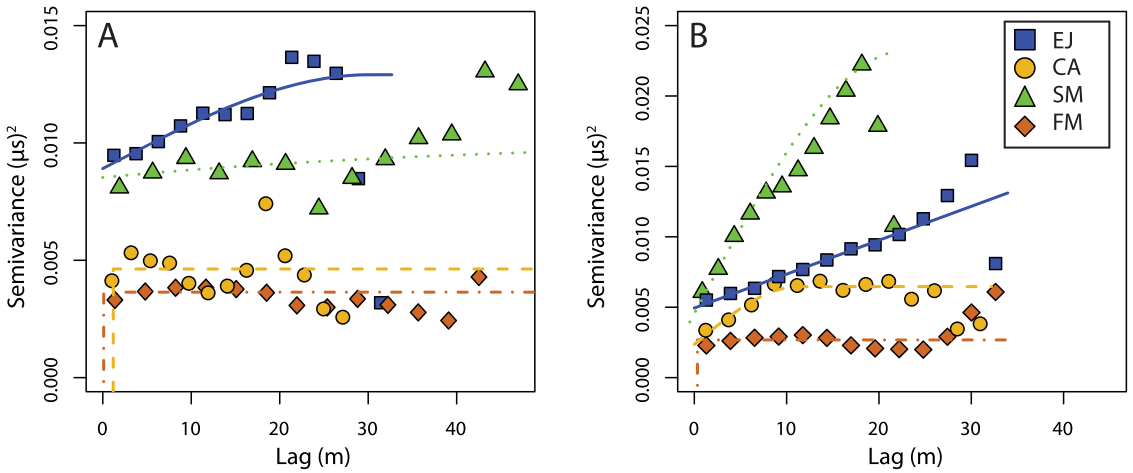

Fig. 6. (A) Dry and (B) wet season semivariance. The lines are the modeled semivariograms, calculated using an omnidirectional variogram with the best fit (Table 4; spherical or exponential, with or without a nugget). None of the sites were spatially correlated during either season for the distances covered by the study.

squares fit than does the exponential model for all but four of the models. For three models (CA during the dry season and FM during the wet and dry seasons), the type of model did not affect the sum-of-squares fit and is listed as Sph/Exp. For SM during the dry season, the exponential model had a lower sum-of-squares fit. We also tested whether the model required a nugget; for all of the models, setting a nugget provided a better model fit than reducing the nugget to zero.

Beyond the presence of a nugget, the semivariogram models (lines) show no consistent trends in autocorrelation related to either season or site wetness and do not fit the calculated semivariance of the measured data well (Fig. 6). In the wet season (right panel), the wet sites' semivariance does not reach a plateau, suggesting that the autocorrelation distance is longer than the measured length of the hillslopes. For the dry season (left panel), the models of the semivariance (lines) fail to capture the calculated semivariance at CA and FM because there is no spatial correlation across the hillslopes.

3.4. Soil hydrologic properties

The results of the MDI experiments measured over the course of one day at each site show that the soils' sorptivity and measured unsaturated hydraulic conductivity (hereafter, K_{unsat}) were heterogeneous during both wet and dry field seasons. We report both values in Table 5 because the sorptivity, which represents a soil's ability to draw water (Stewart et al., 2013), does not depend upon the soil wetness when measured, unlike unsaturated hydraulic conductivity measurements. Because the MDI experiments are completed over very small areas (the diameter of the steel disk applied to the soil surface is 4.5 cm), this heterogeneity is expected, but even in settings with massive spatial variability in hydraulic conductivity, enough measurements with a mini disk can be used to provide useful estimates of effective infiltration capacity at the catchment scale (McGuire et al., 2018). Regardless of the mean soil water content for each hillslope, the unsaturated hydraulic conductivity did not exhibit patterns based on the distance downslope from the datum at each site, suggesting that shallow soil water was not accumulating downslope. We measured the soil saturation at each point prior to running the MDI experiments and saw no relationship between shallow soil saturation, the soil sorptivity, and the unsaturated hydraulic conductivity. Other hydrologic properties at the four sites, including bulk density and calculated porosity, grain size distributions, pH, and the weight percentage of amorphous material, are reported along with the results of the MDI experiments in Table 5. Because we made all of the soil moisture measurements in the upper soil layer, only topsoil (0 − 15 cm, samples from the O or Ah horizons; Lasso and Espinosa, 2018) properties are included. During the dry field season, we collected surface bulk density samples at the same location we made the MDI measurements at FM and EJ; however, there is no apparent relationship between the two properties. The other measured hydrologic properties at FM and EJ have no correlation with the MDI-measured K_{unsat} values at FM and EJ. We compared the K_{unsat} data to the intensity of rainfall during the field seasons for all of the sites (Fig. 7). At all of the sites, the range of measured unsaturated hydraulic conductivity spanned orders of magnitude. The smallest values measured for the unsaturated hydraulic conductivity at each site are within the same order of magnitude of rainfall intensity (Table 5), while the largest values are much higher than the measured rainfall intensity. However, because we avoided obvious macropores (observed at Sitio Mirador, the only site at which surficial expression of the presence of macropores was clear) and adjusted the suction for the MDI to exclude macropore flow, the calculated K_{unsat} values only apply to the soil matrix. Because we did not account for macropore flow in our measurements of K_{unsat}, the precipitation and K_{unsat} values may not overlap at all if macropore flow is important and rapid infiltration through macropores dominates infiltration. Additionally, we calculated the rainfall intensities from the total precipitation collected in a tipping bucket rain gauge and integrated over the data logger's recording time (5 − 15 min). Likely some of the instantaneous rainfall intensities were slightly higher than the values integrated over the relatively short measurement periods.

Table 5
Site-wide values of measured physical properties from surface (0–10 cm) soil samples.

Site	% Sand	% Clay	Surface % % Amorphous*	Bulk density (g cm^{-3})	Calculated porosity	pH	Sorptivity (cm $s^{-1/2}$)	Season	Unsaturated hydraulic conductivity (cm s^{-1})
El Junco (EJ)	29.3 – 67.2	7.3 – 46.7	14.57	0.96 – 1.59[b]59†	0.38 – 0.63	3.77 – 4.99	5.8×10^{-5} – 2.4×10^{-3}	Wet	0
								Dry	8.4×10^{-5} – 0.001 [c]‡
Cerro Alto (CA)	42.1 – 79.5	6.5 – 54.8	3.57	1.08 – 1.23	0.52 – 0.59	5.39 – 6.70	6.7×10^{-5} – 1.4×10^{-4}	Wet	0.00216
								Dry	4.3×10^{-5} - 0.000291 [c]‡
Sitio Mirador (SM)	0 – 87.8	4.3 – 100	7.20	1.03 – 1.46	0.44 – 0.60	5.92 – 6.53	1.4×10^{-5} – 6.5×10^{-4}	Wet	–
								Dry	7.3×10^{-5} – 0.0013
Finca Merceditas (FM)	7.7 – 85.1	4.9 – 88.9	1.63	1.06 – 1.56[b]56†	0.40 – 0.59	5.71 – 6.69	3.0×10^{-4} – 3.6×10^{-2}	Wet	–
								Dry	7.9×10^{-5} – 0.010

*Amorphous material weight percentages were only measured for a single soil pit at each site, so no range is provided. [b]† Samples of saprolite that were found in the soils. [c]‡ Only two values of hydraulic conductivity were measured. – Unsaturated hydraulic conductivity was not measured.

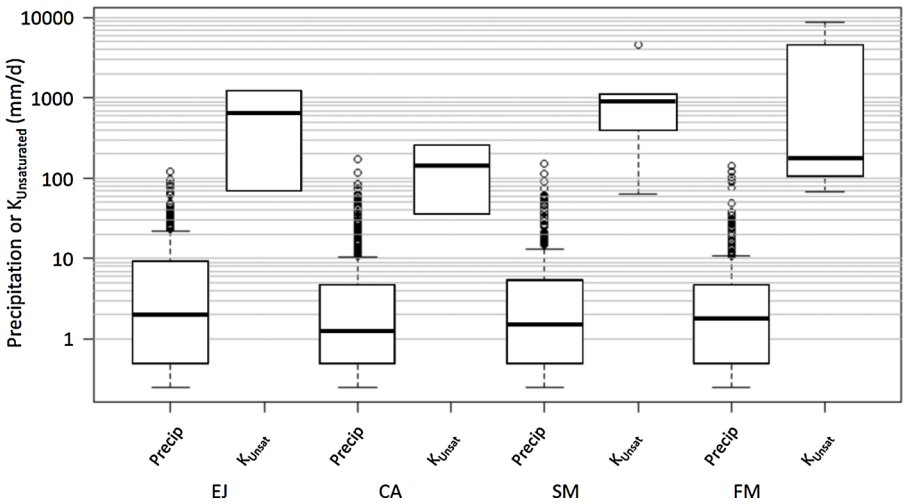

Fig. 7. The comparison between the precipitation and unsaturated hydraulic conductivity measured at each site shows that the means and ranges of precipitation intensity are much smaller than the means and ranges measured for the unsaturated hydraulic conductivity. Note that y-axis, in mm/d, is log scale.

While in the field, we excavated soil pits across the hillslopes; at EJ, we observed water exfiltrating along the O and A horizon boundary in the profile wall (between 8 and 15 cm deep across the entire hillslope) when there was heavy rain (every day during the wet season, one day during the dry season). At CA, we observed water moving along a boundary between less clay-rich and clay-rich layers only during the wet season. At SM and FM, we did not observe water exfiltration from the exposed face of the soil pits. Although numerous studies indicate that saprolite that underlies many tropical sites may have bimodal pore size distributions (Navarre-Sitchler et al., 2013), we observed no evidence of such a distribution within the saprolites from the soil pits.

4. Discussion

4.1. Do the soil water saturation states differ seasonally?

At the three study sites with temporally continuous records of soil saturation (EJ, CA, and FM), we observed changes in the percent saturation for all depths between the wet season and the dry season (Table 6). This shift in the seasonal percent saturation was unsurprisingly supported by changes in the mean soil saturation measured by the two areal studies. EJ had one rain event during the dry season for which there are both temporal and spatial data. Over the course of the event, the soil water saturation of the areal study increased by a percent change of 18.5%, and the soil water saturation measured by the weather station increased by a percent change of 20.3%. With additional spatial surveys and in situ soil moisture probes, determining if the weather stations provide a representative measurement of the change in the percent saturation would be possible.

Table 6
Seasonal variability in mean soil saturation by depth.

Site	Season	Probe depth	Mean % saturation	Variance (σ^2)
El Junco (EJ)	Wet	10 cm	86.3	1.1
		20 cm	85.8	0.4
		40 cm	92.6	0.1
	Dry	10 cm	50.5	2.2
		20 cm	64.2	1.3
		40 cm	84.3	0.2
Cerro Alto (CA)	Wet	10 cm	69.6	1.8
		20 cm	82.5	0.6
		30 cm	90.5	0.3
	Dry	10 cm	31.8	0.1
		20 cm	55.2	0.3
		30 cm	64.9	0.3
Finca Merceditas (FM)	Wet	10 cm	82.8	0.3
		20 cm	57.9	0.1
		30 cm	57.6	0.1
	Dry	10 cm	52.8	0.4
		20 cm	41.2	0.2
		30 cm	41.1	0.1

Because this study fell during an El Niño, the seasonal changes that we described represent extreme cases of wet and dry. The highest intensity and amount of precipitation measured at EJ corresponds to the record of the greatest saturation of soils at all depths. When rainfall declined during the dry season, the calculated reference evapotranspiration was higher and more variable, reflecting an increase in solar radiation and windspeed. El Niño usually results in more convective rainfall and less fog in the Galápagos (Trueman and D'Ozouville, 2010), so it is possible that during non-El Niño years, the soils at EJ do not dry as much as they did during our study period, which occurred during an intense El Niño year. At CA, the rainy periods corresponded to the highest measured soil saturation, while the reference evapotranspiration was variable throughout the year, reflecting the site's leeward position and the fact that it receives less consistent rainfall and fog during dry seasons compared to the windward sites. Because island-wide convective storms are more common during El Niño years, the high soil saturation observed during this study at CA may be uncharacteristic of the site. FM also has a distinct rainy and dry season, although it received more dry season precipitation than the leeward CA. Higher soil saturation was associated with the rainy seasons, but the reference evapotranspiration stayed consistent throughout the year, reflecting the fact that the site receives less precipitation than EJ, but more than CA.

We examined the change in variance in the temporal soil water content record and observed shifts through time. The sites showed different relationships between the saturation state and the variance, with higher measured variance during the dry season at EJ and lower variance during the dry season at CA. The variance around the mean percent saturation at FM remains nearly the same for both seasons. Many authors have observed that the highest variance in soil moisture is associated with mid-range mean soil moisture measurements in near-surface soils (Choi et al., 2007; Famiglietti et al., 2008), although researchers have also noted that variance can both increase or decrease with changes in the mean soil moisture (Pan and Peters-Lidard, 2008). For example, at a temperate site in Virginia (USA), it was noted that the lowest variance around mean soil moisture is associated with extreme wet and dry periods (Lawrence and Hornberger, 2007). The authors determined that during dry periods, the variance is controlled by the wilting point of plants; during temperate periods, the variance is dictated by the hydraulic conductivity of soils; and during wet periods, the variance is controlled by the soil porosity. In the case where authors working in sodic soils observed that while the highest variance was associated with mid-range soil moisture measurements at depths below 20 cm, they still observed that the shallowest soil moisture measurements (0 − 6 cm) exhibited the highest variance associated with the extreme wet and dry soil moisture periods (Peterson et al., 2019). Additionally, their observation of high variance associated with extreme wet and dry values in deeper soils is likely the result of the chemical properties of the soils affecting the conductivity of clay pans at depths greater than 20 cm.

The depth to the point of refusal, which is generally the depth to a clay-rich horizon, is deeper than the shallowest soil moisture probe at each weather station, and the chemistry of the soils do not display sodic characteristics (Percy, 2020), so we assume that the sites' variance decreases as conditions approach extreme wet and dry conditions. To this end, we compared the wet and dry seasons to understand what possible factors may affect the percent saturation at the sites, using Lawrence and Hornberger's (2007) drivers of variance for different saturation states. At EJ, we observed a shift between the wet and dry seasons from lower to higher variance, suggesting a possible shift from the control of soil saturation by maximum soil porosity to the control of the soil saturation by hydraulic conductivity and other hydrologic properties. EJ's surface soil remained more saturated than any of the other sites throughout the year (Table 2), resulting in the plants on the planar hillslope unlikely to demonstrate water stress during any part of the study period. Conversely, the variance in CA declined between the wet and the dry periods, suggesting that CA shifted from a state where soil saturation was controlled by hydrologic factors to a point where the plants' wilting points were being reached. Field observations of dried grasses and herbs support this hypothesis, although matric pressure was not measured so this hypothesis cannot be further tested. The lack of a statistically significant change in the variance at FM led us to conclude that there was not a major shift in what factors are controlling the soil saturation at this site. Conversely, it is possible that the control of the saturation of soils at FM had shifted from porosity to the wilting point of plants, but we find this to be unlikely based on field observations at FM during the dry season, when grasses and herbs were still green, and because the deeper probes rarely recorded full saturation values. Further field campaigns would benefit from a longer temporal record and the installation of additional in situ soil moisture probes to account for variable changes in the percent saturation across the sites.

4.2. Do the spatial patterns of near-surface soil water shift seasonally?

With the spatial surveys of soil moisture, we intended to test whether observable differences in the spatial patterns of near-surface soil moisture (12 cm) across the hillslopes are based on the season. Our findings indicate that the heterogeneity of soil water across the hillslopes remained high during both wet and dry seasons, but based on only two spatial surveys, determining the temporal stability of the heterogeneity is not yet possible. The semivariogram analysis indicates that the autocorrelation distance was longer than the length of the studied hillslopes. The lack of spatial autocorrelation on our measured scales may reflect the size of the hillslopes, their planar morphology, or the heterogeneity of soil properties across the hillslopes. We used simple regressions to test whether topography, depth to refusal, or slope could be used to predict the percent saturation, but no relationship was observed between any of these variables and the spatial soil moisture measurements. We used Wilcoxan signed rank tests to test whether plant type led to distinguishable differences in percent saturation, but differences between plant types were not statistically significant at any of the sites. This suggests that at the scales of the plots in which we worked a combination of these variables affects the surface soil moisture, in addition to the microclimatic conditions associated with each measurement point. Previous studies noted that plot-scale variability in soil moisture can be very high when compared to landscape-scale variability (Kaiser and McGlynn, 2018); because this study was limited to the hillslopes at which weather stations were installed, we did not measure catchment-scale variability in soil water content.

We noted from the temporal soil moisture record that EJ's variance in percent saturation was higher in the dry season than in the

wet season, while CA's variance was lower in the dry season than in the wet season, and FM's variance was the same throughout the seasons (Section 4.1). However, the variance from the spatial soil moisture measurements from the seasonal surveys was consistently higher during the dry season compared to the wet season. Although the temporal and spatial variance are not directly comparable because of the nature of the study design, the dry season's higher spatial variance may be due to surface soils drying and approaching wilting points.

Reasons why the spatial patterns of soil water remained highly heterogeneous throughout both seasons are numerous, despite differences in stochastic variables like precipitation and evapotranspiration. Previous work completed across a much larger catchment at Tarrawarra (Victoria, Australia) noted a change in the heterogeneity of spatial soil moisture observations between the wet and dry season, with soil water content increasing in the convergent portions of the catchment during wet periods (Western and Grayson, 1998, 2000). The planar nature of the studied hillslopes, coupled with their small size, make it unlikely that we captured sufficient data in convergent areas where flowlines meet, possibly explaining the lack of recorded seasonal reorganization of soil water.

Additionally, the interpretation of the spatial distribution of soil water is convoluted by the fact that each site's soil water survey took several days to complete. The weather stations were installed after we completed the spatial surveys in the wet season, so we are unable to show the change in soil water content through time for the first spatial survey; however, we can show how the soil moisture changed during the dry season over the course of the surveys (Fig. S4). At FM and CA, the weather station recorded a mean value of volumetric water content of 29.7% and 25.4%, respectively, with a standard deviation of 0.2% over the time period during which we collected spatial data. However, a rainstorm at EJ on one of our measurement days caused the soil water content to rise and the resulting standard deviation of the soil water measured at the weather station during the four days of the spatial survey is an order of magnitude higher at EJ (2.3%) compared to FM and CA. Further surveys of spatial distributions of soil water will benefit from single-day collection, which was not possible with the limited resources and narrow scope of this project.

4.3. Do spatial patterns of soil water affect runoff generation?

Despite intense rainfall at all of the sites during the rainy season, we did not observe evidence of connected surface runoff across the studied hillslopes at EJ, SM, and FM, including little evidence of gully formation at the agricultural sites or bottom-slope wetness. The only runoff that we observed was at CA along a cow trail, and then only when the trail passed beneath a basalt bluff. Based on the spatial distribution of soil moisture across the hillslopes and the semivariogram analyses of the spatial distributions, we propose that the lack of runoff at the four sites is due to low spatial connectivity across each hillslope and variable responses to wetting and drying at different depths of the soil, coupled with generally high hydraulic conductivity in surface soils. The low spatial connectivity of the surface soil water, identified using semivariogram analysis, affected runoff because the amount of water in soils varied spatially. From the temporal record of soil water content, we noted variable responses to wetting and drying between the surface soil probes (10 cm) and the deeper soil moisture measurements made within the root zone. The delays between the arrival of water at the surface soil probe and the deeper probes suggest vertical infiltration is largely matrix-flow dominated. We also observed a large range of sorptivity and unsaturated hydraulic conductivity (Fig. 7, Table 5). The range of the unsaturated hydraulic conductivities (Table 5) suggests that some parts of the hillslopes were more conductive than others. From the MDI experiments, we know these areas may be very close to one another (within 1 m).

Incorporating the observations of spatial and vertical heterogeneity, we propose two possible explanations for the lack of runoff observed at the sites. The first is that highly permeable, unsealed surface material distributed across the hillslopes allows water to vertically infiltrate into the soil column. Previous authors modeling arid and semiarid catchments found that the sealing status of the shallowest portions of a soil profile were a more important factor in generating runoff than spatial heterogeneity (Assouline and Mualem, 2006). They showed that simulations of catchments with no surface seal formation generated little cumulative runoff. However, this explanation does not fit our observations, as we did not observe soil sealing on any of the hillslopes, and the hydrologic properties and soil water distributions are highly heterogeneous at each site. Instead of uniform, highly permeable soil surfaces, we suggest that surface soil that becomes saturated simply becomes a source of soil water to adjacent soil that is less saturated and can accommodate the excess water by serving as a sink. The high variability in unsaturated hydraulic conductivity provides further evidence that intense precipitation does not saturate a soil and start flowing overland because areas with lower soil moisture and higher hydraulic conductivity are nearby and can serve as sinks for excess water. This supports the hypothesis of more "transmissive" and "retentive" parts of the hillslopes that prevent the accumulation of observable and measurable overland flow across hillslopes. Thus, any patches of runoff are not connected with another downslope and limit the occurrence and impacts of overland flow.

Transmissive soils conduct water more easily when wet (higher hydraulic conductivities), while retentive soils conduct water poorly when wet (lower hydraulic conductivities) but can retain soil moisture for longer periods of time. High-intensity rainfall may produce localized runoff from retentive soils that infiltrates into adjacent parcels of more transmissive soil (Nimmo et al., 2009). On San Cristóbal, this model may explain the lack of runoff on the planar hillslopes: because of the high heterogeneity in hillslope-scale characteristics, like soil texture and the amount of amorphous material, both of which affect hydraulic conductivity, parcels of transmissive and retentive soils may be adjacent to each other. The lack of autocorrelation across small distances (less than 100 m) on the hillslopes provides support for this model of a patchwork of transmissive and retentive soils.

Runoff generation at temperate sites may depend on whether lateral or vertical flow paths are dominant along the hillslopes, where the presence of lateral flow paths depends on the morphology of the landscape (Elsenbeer, 2001; Fitzjohn et al., 1998). For our study, none of the studied slopes featured gullies or other areas of high convergence (Fig. S1), so it is unlikely that large amounts of surface lateral flow were driven by hillslope morphology. At CA, the uppermost portion of the site was saddle shaped and crisscrossed

by cow paths. Soil water may have accumulated due to lateral flow in the slightly convergent portion of the saddle (Fig. 4), but the remainder of the data from the spatial survey at the site demonstrated no similar accumulation. Most soil water evaporates directly from the soil surface, is used by plants, or infiltrates vertically until the water reaches an aquitard and begins to flow laterally. In excavated soil pits during the wet season, we observed water seeping out of the upslope walls along the horizon boundaries, supporting lateral redistribution of water at depth. At CA, also a "water meadow" at the base of a nearby hillslope wetted after small rain events, despite no evidence of runoff along the hillslope, supporting the idea that water may be laterally redistributed deeper within the soil.

Our hypothesis to explain the lack of observed surface runoff on the hillslopes corroborates work completed on other tropical ocean islands. On the island of Santa Cruz, Galápagos (to the west of San Cristóbal), soil profiles were instrumented with tensiometers to measure the pressure head within soil profiles under two different land cover types (forest, pasture; Domínguez et al., 2016). Those data were then incorporated into a soil water transfer model, which showed that runoff was negligible because the soil water input never exceeded the infiltration capacity of the soils, as we observed at the sites on San Cristóbal. Based on the model, deep percolation into the groundwater system occurred in both land use regimes, suggesting that vertical flow paths through the soil results in groundwater recharge. Previous work on Hawaii observed a similar phenomenon—the surface soil had little connectivity, resulting in negligible runoff, but after vertical infiltration, lateral redistribution of soil water was observed at horizon boundaries due to the change in the hydraulic conductivity between different horizons (Lohse and Dietrich, 2005). Future work on San Cristóbal should include the measurement of hydraulic conductivity across broader areas and in different horizons to better characterize spatial variations in conductivity that control runoff and groundwater recharge.

4.4. Soil water and island-wide hydrogeology

Previous work on the hydrogeology of San Cristóbal has related the island's groundwater system to that of Hawaii (Violette et al., 2014). Consecutive lava flows, separated by baked paleosols or tuffs, have led to a complicated groundwater system of perched aquifers, some of which drain to a basalt aquifer and some that result in springs. This is similar to the hydrogeology of many other basalt systems, including continental basalts like those found on the Snake River Plain (Mirus et al., 2011) and other ocean islands, like Piton de la Fournaise on La Reúnion (Violette et al., 1997). San Cristóbal is the only island in the archipelago with multiple perennial streams, maintained by springs that drain the perched aquifers. This understanding has come through geophysical (Adelinet et al., 2018; Auken et al., 2009; Pryet et al., 2012a) and geochemical (Warrier et al., 2012) observations.

Little research has previously connected inputs into the island's hydrologic system with the groundwater system. From this study, we propose that water that has been transmitted through the soil's root zone and into the deeper horizons of the soil will either flow laterally along horizons of low hydraulic conductivity, resulting in high soil water contents and seeps that emerge in areas of convergence (like the water meadow at the base of CA), or will infiltrate further through the unconsolidated saprolite to enter the deeper groundwater system. Due to the lack of monitoring wells on San Cristóbal, exact determination of the amount of infiltrated water that enters the groundwater system is unknown, but the research on the behavior of surface and root zone soil water helps provide an important step in further understanding water cycling on San Cristóbal. This study is far from comprehensive, but the data provide ample opportunities for further testing of conceptual and numerical models of hillslope hydrologic response on San Cristóbal and similar tropical island settings. Additional efforts must also be made to improve instrumentation of hillslopes in diverse climates across San Cristóbal to track how seasonality affects the distribution and behavior of soil water.

5. Conclusions

We have compared the temporal and spatial records of soil water on four planar hillslopes on San Cristóbal, Galápagos, to develop a qualitative model of water in near-surface soils in different climate zones. This work aims to provide a component of our understanding of the hydrogeology of San Cristóbal, and possibly, other ocean islands. We initially sought to answer three questions: (1) does soil water differ seasonally; (2) does the spatial distribution of soil water differ through time; and (3) could spatial patterns of soil water affect runoff generation. The findings of this study confirm that temporal differences in saturation states on the studied hillslopes are driven by seasonal differences in precipitation and evapotranspiration, and the position of the hillslopes on San Cristóbal's climosequence and their windward/leeward position. Thus, our dataset is a valuable resource for future hydrologic and soil-atmosphere modeling efforts. We complemented the temporal differences in saturation state with surveys of the spatial variability of the soil water across the studied hillslopes, showing that during both wet and dry seasons, the soil water content was highly variable spatially and randomly distributed across the hillslope. This spatial variability is likely the result of the heterogeneity of a number of factors, including physical and hydrologic characteristics of the soil and the microclimate and microtopography around each of the measurement points. While in the field, we did not observe evidence of runoff at most of the sites except along the cow path at CA, despite numerous heavy rain events. Because near-surface soil moisture was not spatially connected and the hydraulic conductivity is higher than rainfall intensity, we conclude that retentive patches of soil which can generate runoff are adjacent to transmissive patches of soil. Transmissive soils have higher hydraulic conductivities and can transmit potential runoff into deeper horizons of the soil system. This may explain observations that uncultivated hillslopes on San Cristóbal have little surface-runoff connectivity, as well as explaining how water enters the shallow groundwater system that is drained by numerous springs.

Fieldwork in the Galápagos remains challenging, and our measurement and monitoring campaigns were restricted by access and resources. Our results confirm what might be presumed based on initial site assessments and field trips, namely that seasonal changes in precipitation and elevation-dependent precipitation inputs affect the soil saturation across the sites. However, our study provides

concrete evidence to support the conceptual model for hillslope hydrology on San Cristóbal. These baseline data can be expanded to improve our understanding of the behavior of water through the surface soil across San Cristóbal's climate gradient. Additional fieldwork on the hillslopes can capture the spatial distribution of soil water across the hillslopes with different precipitation inputs to accurately model the temporal stability of soil moisture distributions. The installation of more research infrastructure, especially piezometers and additional soil water probes at different points across the currently instrumented sites, will yield valuable information to help track the fate of soil water that infiltrates beneath the clay layer at each site. Testing soil-water models using the data presented in this paper can also facilitate improved quantitative understanding of factors affecting the distribution of soil water across the hillslopes, as well as predict the fate of the soil water through the water cycle on the island.

Acknowledgments

This work was supported by a NSF Graduate Research Fellowship grant (DGE-1650116), a Geological Society of America Student Research Grant (10804-15), the NSF Science Across Virtual Institutions International Critical Zone Observatory Grant, and UNC's Department of Geological Sciences Martin Fundawarded to M.S. Percy. All the data described in this work can be obtained by emailing the corresponding author (madelynp@live.unc.edu). The authors appreciate logistical collaboration with the UNC-USFQ Galápagos Science Center, particularly Leandro Vaca and Juan Pablo Muñoz. We thank Juliana Borja, Rebecca Chaisson, Sara Guevara, Claris Orellana, Sarah Schmitt, Kayla Seiffert, and Erin VanderJeudgt for field assistance. The manuscript benefited enormously from feedback provided by Kim Perkins of the U.S. Geological Survey and two anonymous reviewers. Any use of trade, firm, or product names is for descriptive purposes only and does not imply endorsement by the U.S. Government.

Appendix A. Supplementary data

Supplementary material related to this article can be found, in the online version, at doi:https://doi.org/10.1016/j.ejrh.2020.100692.

References

Adelinet, M., Domínguez, C., Fortin, J., Violette, S., 2018. Seismic-refraction field experiments on Galapagos Islands: a quantitative tool for hydrogeology. J. Appl. Geophys. 148, 139–151. https://doi.org/10.1016/j.jappgeo.2017.10.009.

Assouline, S., Mualem, Y., 2006. Runoff from heterogeneous small bare catchments during soil surface sealing. Water Resour. Res. 42, W12405. https://doi.org/10.1029/2005WR004592.

Auken, E., Violette, S., D'Ozouville, N., Deffontaines, B., Sorensen, K.I., Viezzoli, A., de Marsily, G., 2009. An integrated study of the hydrogeology of volcanic islands using helicopter borne transient electromagnetic: application in the Galapagos archipelago. C.R. Geosci. 341, 899–907. https://doi.org/10.1016/j.crte.2009.07.006.

Bailey, S.W., Brousseau, P.A., McGuire, K.J., Ross, D.S., 2014. Influence of landscape position and transient water table on soil development and carbon distribution in a steep, headwater catchment. Geoderma 266–227, 279–289. https://doi.org/10.1016/j.geoderma.2014.02.017.

Beven, K.J., Kirkby, M.J., 1979. A physically based, variable contributing area model of basin hydrology. Hydrol. Sci. Bull. 24, 43–69. https://doi.org/10.1080/02626667909491834.

Bi, H., Li, X., Liu, X., Guo, M., Li, J., 2009. A case study of spatial heterogeneity of soil moisture in the Loess Plateau, western China: a geostatistical approach. Int. J. Sediment. Res. 24, 63–73. https://doi.org/10.1016/S1001-6279(09)60016-0.

Blake, G.R., Hartge, K.H., 1986. Bulk density. In: Klute, A. (Ed.), Methods of Soil Analysis, Part 1 Physical and Mineralogical Methods. American Society of Agronomy, Madison, WI, pp. 363–376.

Brocca, L., Melone, F., Moramarco, T., Morbidelli, R., 2009. Soil moisture temporal stability over experimental areas in Central Italy. Geoderma 148, 364–374. https://doi.org/10.1016/j.geoderma.2008.11.004.

Chandler, K.R., Stevens, C.J., Binley, A., Keith, A.M., 2018. Influence of tree species and forest land use on soil hydraulic conductivity and implications for surface runoff generation. Geoderma 310, 120–127. https://doi.org/10.1016/j.geoderma.2017.08.011.

Choi, M., Jacobs, J.M., Cosh, M.H., 2007. Scaled spatial variability of soil moisture fields. Geophys. Res. Lett. 34, L01401. https://doi.org/10.1029/2006GL028247.

Colinvaux, P.A., 1972. Climate and the Galapagos islands. Nature 240, 17–20. https://doi.org/10.1038/240017a0.

D'Ozouville, N., Auken, E., Sorensen, K.I., Violette, S., de Marsily, G., Deffontaines, B., Merlen, G., 2008a. Extensive perched aquifer and structural implications revealed by 3D resistivity mapping in Galapagos volcano. Earth Planet. Sci. Lett. 269, 518–522. https://doi.org/10.1016/j.epsl.2008.03.011.

D'Ozouville, N., Deffontaines, B., Benveniste, J., Wegmüller, U., Violette, S., de Marsily, G., 2008b. DEM generation using ASAR (ENVISAT) for addressing the lack of freshwater ecosystems management, Santa Cruz Island, Galapagos. Remote Sens. Environ. 112, 4131–4147. https://doi.org/10.1016/j.rse.2008.02.017.

Dari, J., Morbidelli, R., Saltalippi, C., Massari, C., Brocca, L., 2019. Spatial-temporal variability of soil moisture: addressing the monitoring at the catchment scale. J. Hydrol. (Amst.) 570, 436–444. https://doi.org/10.1016/j.jhydrol.2019.01.014.

Domínguez, C., Pryet, A., García Vera, M., Gonzalez, A., Chaumont, C., Tournebize, J., Villacís, M., D'Ozouville, N., Violette, S., 2016. Comparison of deep percolation rates below contrasting land covers with a joint canopy and soil model. J. Hydrol. (Amst.) 532, 65–79. https://doi.org/10.1016/j.jhydrol.2015.11.022.

Domínguez, C.G., García Vera, M.F., Chaumont, C., Tournebize, J., Villacís, M., D'Ozouville, N., Violette, S., 2017. Quantification of cloud water interception in the canopy vegetation from fog gauge measurements. Hydrol. Process. 31, 3191–3205. https://doi.org/10.1002/hyp.11228.

Dong, J., Ochsner, T.E., 2018. Soil texture often exerts a stronger influence than precipitation on mesoscale soil moisture patterns. Water Resour. Res. 54, 2199–2211. https://doi.org/10.1002/2017WR021692.

Ebel, B.A., 2013. Simulated unsaturated flow processes after wildfire and interactions with slope aspect. Water Resour. Res. 49, 8090–8107. https://doi.org/10.1002/2013WR014129.

Elsenbeer, H., 2001. Hydrologic flowpaths in tropical rainforest soilscapes–a review. Hydrol. Process. 15, 1751–1759. https://doi.org/10.1002/hyp.237.

Esri, 2011. ArcGIS Desktop.

Famiglietti, J.S., Ryu, D., Berg, A.A., Rodell, M., Jackson, T.J., 2008. Field observations of soil moisture variability across scales. Water Resour. Res. 44, W01423. https://doi.org/10.1029/2006WR005804.

Fitzjohn, C., Ternan, J.L., Williams, A.G., 1998. Soil moisture variability in a semi-arid gully catchment: implications for runoff and erosion control. Catena 32, 55–70. https://doi.org/10.1016/S0341-8162(97)00045-3.

Foster, D., Swanson, F., Aber, J., Burke, I., Brokaw, N., Tilman, D., Knapp, A., 2003. The importance of land-use legacies to ecology and conservation. Bioscience 53, 77–88. https://doi.org/10.1641/0006-3568(2003)053[0077:TIOLUL]2.0.CO;2.

Gao, L., Wang, Y., Geris, J., Hallett, P.D., Peng, X., 2019. The role of sampling strategy on apparent temporal stability of soil moisture under subtropical hydroclimatic

conditions. J. Hydrol. Hydromech. 67, 260–270. https://doi.org/10.2478/johh-2019-0006.
Geist, D.J., McBirney, A.R., Duncan, R.A., 1986. Geology and petrogenesis of lavas from San Cristóbal Island, Galapagos Archipelago. Geol. Soc. Am. Bull. 97, 555–566. https://doi.org/10.1130/0016-7606(1986)97<555:GAPOLF>2.0.CO;2.
Geist, D.J., Snell, H., Snell, H., Goddard, C., Kurz, M.D., 2014. A paleogeographic model of the galápagos Islands and biogeographic and evolutionary implications. In: Harpp, K., Mittelstaedt, E., D'Ozouville, N., Graham, D.W. (Eds.), The Galapagos: A Natural Laboratory for the Earth Sciences. Wiley Press, Washington D.C, pp. 167–183.
Graham, R.C., Rossi, A.M., Hubbert, K.R., 2010. Rock to regolith conversion: producing hospitable substrates for terrestrial organisms. GSA Today 20, 4–9. https://doi.org/10.1130/GSAT57A.1.
Grayson, R.B., Western, A.W., Chiew, F.H.S., Bloschl, G., 1997. Preferred states in spatial soil moisture patterns: local and nonlocal controls. Water Resour. Res. 33, 2897–2908. https://doi.org/10.1029/97WR02174.
Hu, S., Fedorov, A.V., 2019. The extreme El Niño of 2015-2016: the role of westerly and easterly wind bursts, and preconditioning by the failed 2014 event. Clim. Dyn. 52, 7339–7357. https://doi.org/10.1007/s00382-017-3531-2.
Huttel, C., 1986. Zonificación bioclimatológica y formaciones vegetales en las Islas Galápagos. Cult. Banco Cent. Ecuador 24, 1–13.
Jackson, M.L., Lim, C.H., Zelazny, L.W., 1986. Oxides, hydroxides, and aluminosilicates. In: Klute, A. (Ed.), Methods of Soil Analysis, Part 1 Physical and Mineralogical Methods. American Society of Agronomy, Madison, WI, pp. 101–150.
Kaiser, K.E., McGlynn, B.L., 2018. Nested scales of spatial and temporal variability of soil water content across a semiarid montane catchment. Water Resour. Res. 54https://doi.org/10.1029/2018WR022591. 21 pp.
Lasso, L., Espinosa, J., 2018. Soils from the galapagos Islands. In: Espinosa, J. (Ed.), The Soils of Ecuador. Springer International Publishing, Berlin, pp. 139–150. https://doi.org/10.1007/978-3-319-25319-0_5.
Lawrence, J.E., Hornberger, G.M., 2007. Soil moisture variability across climate zones. Geophys. Res. Lett. 4, 1–5. https://doi.org/10.1029/2007GL031382.
Lohse, K.A., Dietrich, W.E., 2005. Contrasting effects of soil development on hydrological properties and flow paths. Water Resour. Res. 41, 1–17. https://doi.org/10.1029/2004WR003403.
Martinez, C., Hancock, G.R., Kalma, J.D., Wells, T., 2008. Spatio-temporal distribution of near-surface and root zone soil moisture at the catchment scale. Hydrol. Process. 22, 2699–2714. https://doi.org/10.1002/hyp.6869.
McGuire, K.J., McDonnell, J.J., Weiler, M., Kendall, C., McGlynn, B.L., Welker, J.M., Seibert, J., 2005. The role of topography on catchment-scale water residence time. Water Resour. Res. 41, W05002. https://doi.org/10.1029/2004WR003657.
McGuire, L.A., Rengers, F.K., Kean, J.W., Staley, D.M., Mirus, B.B., 2018. Incorporating spatially heterogeneous infiltration capacity into hydrologic models with applications for simulating post-wildfire debris flow initiation. Hydrol. Process. 32, 1173–1187. https://doi.org/10.1002/hyp.11458.
Metzger, J.C., Wutzler, T., Valle, N.D., Filipzik, J., Grauer, C., Lehmann, R., Roggenbuck, M., Schelhorn, D., Weckmüller, J., Küsel, K., Totsche, K.U., Trumbore, S.E., Hildebrandt, A., 2017. Vegetation impacts soil water content patterns by shaping canopy water fluxes and soil properties. Hydrol. Process. 31, 3783–3795. https://doi.org/10.1002/hyp.11274.
Mirus, B.B., Loague, K., 2013. How runoff begins (and ends): characterizing hydrologic response at the catchment scale. Water Resour. Res. 49, 2987–3006. https://doi.org/10.1002/wrcr.20218.
Mirus, B.B., Perkins, K.S., Nimmo, J.R., 2011. Assessing controls on perched saturated zones beneath the Idaho nuclear technology and engineering center, Idaho. U.S. Geological Survey Scientific Investigations Report 2011-5222. https://doi.org/10.3133/sir20115222.
Navarre-Sitchler, A.K., Cole, D.R., Rother, G., Jin, L., Buss, H.L., Brantley, S.L., 2013. Porosity and surface area evolution during weathering of two igneous rocks. Geochim. Cosmochim. Acta 109, 400–413. https://doi.org/10.1016/j.gca.2013.02.012.
Nimmo, J.R., Perkins, K.S., Schmidt, K.M., Miller, D.M., Stock, J.D., Singha, K., 2009. Hydrologic characterization of desert soils with varying degrees of pedogenesis: I. Field experiments evaluating plant-relevant soil water behavior. Vadose Zone J. 8, 480–495. https://doi.org/10.2136/vzj2008.0052.
Noborio, K., 2001. Measurement of soil water content and electrical conductivity by time domain reflectometry: a review. Comput. Electron. Agric. 31, 213–237. https://doi.org/10.1016/S0168-1699(00)00184-8.
Pan, F., Peters-Lidard, C.D., 2008. On the relationship between mean and variance of soil moisture fields. J. Am. Water Resour. Assoc. 44, 235–242. https://doi.org/10.1111/j.1752-1688.2007.00150.x.
Pansu, M., Gautheyrou, J., 2006. Handbook of Soil Analysis. Springer International Publishing, Berlin.
Pelletier, J.D., Barron-Gafford, G.A., Gutiérrez-Jurado, H., Hinckley, E.-L.S., Istanbulluoglu, E., McGuire, L.A., Niu, G.-Y., Poulos, M.J., Rasmussen, C., Richardson, P., Swetnam, T.L., Tucker, G.E., 2018. Which way do you lean? Using slope aspect variations to understand Critical Zone processes and feedbacks. Earth Surf. Process. Landforms 43, 1133–1154. https://doi.org/10.1002/esp.4306.
Percy, M.S., 2020. Weathering of Tholeiitic Basalt in a Tropical Island System: Effects on Soil Moisture, Soil Processes, and Nutrient Cycling. University of North Carolina at Chapel Hill.
Percy, M.S., Schmitt, S.R., Riveros-Iregui, D.A., Mirus, B.B., 2016. The Galápagos archipelago: a natural laboratory to examine sharp hydroclimatic, geologic and anthropogenic gradients. Wiley Interdiscip. Rev. Water 3, 587–600. https://doi.org/10.1002/wat2.1145.
Peterson, A.M., Helgason, W.H., Ireson, A.M., 2019. How spatial patterns of soil moisture dynamics can explain field-scale soil moisture variability: observations from a sodic landscape. Water Resour. Res. 55, 4410–4426. https://doi.org/10.1029/2018WR023329.
Pryet, A., D'Ozouville, N., Violette, S., Deffontaines, B., Auken, E., 2012a. Hydrogeological settings of a volcanic island (San Cristóbal, Galapagos) from joint interpretation of airborne electromagnetics and geomorphological observations. Hydrol. Earth Syst. Sci. Discuss. 16, 4571–4579. https://doi.org/10.5194/hess-16-4571-2012.
Pryet, A., Dominguez, C., Tomai, P.F., Chaumont, C., D'Ozouville, N., Villacís, M., Violette, S., 2012b. Quantification of cloud water interception along the windward slope of Santa Cruz Island, Galapagos (Ecuador). Agric. For. Meteorol. 161, 94–106. https://doi.org/10.1016/j.agrformet.2012.03.018.
R Core Team, 2017. R: a Language and Environment for Statistical Computing.
Rasmussen, C., Troch, P.A., Chorover, J., Brooks, P., Pelletier, J.D., Huxman, T.E., 2011. An open system framework for integrating critical zone structure and function. Biogeochemistry 102, 15–29. https://doi.org/10.1007/s10533-010-9476-8.
Regalado, C.M., Muñoz Carpena, R., Socorro, A.R., Hernández Moreno, J.M., 2003. Time domain reflectometry models as a tool to understand the dielectric response of volcanic soils. Geoderma 117, 313–330. https://doi.org/10.1016/S0016-7061(03)00131-9.
Ribeiro Jr., P.J., Diggle, P.J., 2001. geoR: A Package for Geostatistical Analysis.
Rosenbaum, U., Bogena, H.R., Herbst, M., Huisman, J.A., Peterson, T.J., Weuthen, A., Western, A.W., Vereecken, H., 2012. Seasonal and event dynamics of spatial soil moisture patterns at the small catchment scale. Water Resour. Res. 48, 1–22. https://doi.org/10.1029/2011WR011518.
Schmitt, S.R., Riveros-Iregui, D.A., Hu, J., 2018. The role of fog, orography, and seasonality on precipitation in a semiarid, tropical island. Hydrol. Process. 32, 2792–2805. https://doi.org/10.1002/hyp.13228.
Schoeneberger, P.J., Wyscoki, D.A., Benham, E.C., Staff, S.S., 2012. Field book for describing and sampling soils. Version 3.0. Natural Resources Conservation Serivce. National Soil Survey Center, Lincoln, NE.
Soil Survey Staff, 2014. Kellogg Soil Survey Laboratory Methods Manual. Soil Survey Investigations Report No. 42, Version 5.0. U.S. Department of Agriculture, Natural Resources Conservation Service.
Starks, P.J., Heathman, G.C., Jackson, T.J., Cosh, M.H., 2006. Temporal stability of soil moisture profile. J. Hydrol. (Amst.) 324, 400–411. https://doi.org/10.1016/j.jhydrol.2005.09.024.
Stewart, R.D., Rupp, D.E., Abou Najm, M.R., Selker, J.S., 2013. Modeling effect of initial soil moisture on sorptivity and infiltration. Water Resour. Res. 49, 7037–7047. https://doi.org/10.1002/wrcr.20508.
Takagi, K., Lin, H.S., 2012. Changing controls of soil moisture spatial organization in the Shale Hills Catchment. Geoderma 173–174, 289–302. https://doi.org/10.1016/j.geoderma.2011.11.003.
Topp, G.C., Davis, J.L., Annan, A.P., 1980. Electromagnetic determination of soil water content: measurements in coaxial transmission lines. Water Resour. Res. 16,

574–582. https://doi.org/10.1029/WR016i003p00574.
Trueman, M., D'Ozouville, N., 2010. Characterizing the Galapagos terrestrial climate in the face of global climate change. Galapagos Res. 67, 26–37.
Tuller, M., Or, D., 2005. Water retention and characteristic curve. Encycl. Soils Environ. https://doi.org/10.1016/B0-12-348530-4/00376-3.
Vachaud, G., Passerat de Silans, A., Balabanis, P., Vauclin, M., 1985. Temporal stability of spatially measured soil water probability density function. Soil Sci. Soc. Am. J. 49, 822–828. https://doi.org/10.2136/sssaj1985.03615995004900040006x.
Violette, S., Ledoux, E., Goblet, P., Carbonnel, J.-P., 1997. Hydrologic and thermal modeling of an active volcano: the Piton de la Fournaise. Reunion. J. Hydrol. 191, 37–63.
Violette, S., D'Ozouville, N., Pryet, A., Deffontaines, B., Fortin, J., Adelinet, M., 2014. Hydrogeology of the galapagos archipelago: an integrated and comparative approach between islands. In: Harpp, K.S., Mittelstaedt, E., D'Ozouville, Noémi, Graham, D.W. (Eds.), The Galapagos: A Natural Laboratory for the Earth Sciences. Wiley Press, Washington D.C, pp. 167–183.
Warrier, R.B., Castro, M.C., Hall, C.M., 2012. Recharge and source-water insights from the Galapagos Islands using noble gases and stable isotopes. Water Resour. Res. 48, 1–19. https://doi.org/10.1029/2011WR010954.
Western, A.W., Blöschl, G., 1999. On the spatial scaling of soil moisture. J. Hydrol. (Amst) 217, 203–224. https://doi.org/10.1016/S0022-1694(98)00232-7.
Western, A.W., Grayson, R.B., 1998. The Tarrawarra data set: soil moisture patterns, soil characteristics, and hydrological flux measurements. Water Resour. Res. 34, 2765–2768. https://doi.org/10.1029/98WR01833.
Western, A.W., Grayson, R.B., 2000. Soil moisture and runoff processes at tarrawarra. In: Grayson, R.B., Blöschl, G. (Eds.), Spatial Patterns in Catchment Hydrology: Observations and Modelling. Cambridge University Press, Cambridge, UK, pp. 209–246.
Western, A.W., Grayson, R.B., Green, T.R., 1999. The Tarrawarra project: high resolution spatial measurement, modelling and analysis of soil moisture and hydrological response. Hydrol. Process. 13, 633–652. https://doi.org/10.1002/(SICI)1099-1085(19990415)13:5<633::AID-HYP770>3.0.CO;2-8.
Western, A.W., Grayson, R.B., Blöschl, G., 2002. Scaling of soil moisture: a hydrologic perspective. Annu. Rev. Earth Planet. Sci. 30, 149–180. https://doi.org/10.1146/annurev.earth.30.091201.140434.
Western, A.W., Zhou, S.-L., Grayson, R.B., McMahon, T.A., Blöschl, G., Wilson, D.J., 2004. Spatial correlation of soil moisture in small catchments and its relationship to dominant spatial hydrological processes. J. Hydrol. (Amst) 286, 113–134. https://doi.org/10.1016/j.jhydrol.2003.09.014.
Zhu, J., Mohanty, B.P., 2003. Upscaling of hydraulic properties of heterogeneous soils. In: Pachepsky, Y., Radcliffe, D.E., Selim, H.M. (Eds.), Scaling Methods in Soil Physics. CRC Press, Boca Raton, pp. 97–117.
Zotarelli, L., Dukes, M.D., Romero, C.C., Migliaccio, K.W., Morgan, K.T., 2010. Step by step calculation of the Penman-Monteith Evapotranspiration (FAO-56 Method). Gainesville, FL.